Journal of Physics: Conference Series

PAPER • **OPEN ACCESS**

Frequency-Dependent Aerodynamic Damping and Inertia in Linearized Dynamic Analysis of Floating Wind Turbines

To cite this article: Carlos Eduardo S Souza *et al* 2020 *J. Phys.: Conf. Ser.* **1452** 012040

View the article online for updates and enhancements.

IOP ebooks™

Bringing you innovative digital publishing with leading voices to create your essential collection of books in STEM research.

Start exploring the collection - download the first chapter of every title for free.

This content was downloaded from IP address 129.241.141.64 on 08/03/2020 at 11:27

Frequency-Dependent Aerodynamic Damping and Inertia in Linearized Dynamic Analysis of Floating Wind Turbines

Carlos Eduardo S Souza, John Marius Hegseth and Erin E Bachynski
Department of Marine Technology, Norwegian University of Science and Technology, 7491 Trondheim, Norway

E-mail: carlos.souza@ntnu.no

Abstract. In frequency-domain (FD) models of floating wind turbines (FWT), it is common to regard the interaction between nacelle motions and thrust by means of a constant aerodynamic damping coefficient. This approach is effective at higher motions frequencies, but does not consider interactions between nacelle motions and the blade pitch control system. As a result, the motions and loads at frequencies closer to the controller bandwidth may be underpredicted. A remedy for this problem is to include the linearized thrust expression in the FD model, such that the dynamic effects related to control are considered. In this paper, these dynamic effects are related to frequency-dependent damping and inertia terms. Expressions for damping and inertia coefficients are obtained with two different methods, and then included in the FD model. The resulting responses are compared to those obtained with the constant damping coefficient method, and also with coupled time-domain simulations of a semi-submersible 10 MW FWT. The better performance of the FD model with frequency-dependent inertia and damping coefficients encourages the adoption of the linearized thrust approach for representing the interaction between nacelle motions, thrust and control system.

1. Introduction

Frequency-domain (FD) methods can be helpful in the design of floating wind turbines (FWTs), providing responses for a large number of loading conditions with relatively low computational time. Previous work has indicated that the response of FWTs in moderate environmental conditions may be estimated reasonably well using FD models [1, 2, 3]. However, their reliability depends on an accurate prediction of loads and interactions with linearized models.

An especially interesting interaction takes place between nacelle motions and the rotor thrust. Fluctuations in the nacelle's horizontal velocity provoke changes in the flow through the rotor, leading to oscillations in the rotor speed and thrust. An aerodynamic damping effect results from this interaction, and is normally included in FD models by means of a constant aerodynamic damping coefficient. This coefficient may be obtained from the thrust derivative w.r.t. the relative wind speed [1, 3, 4], or by means of decay simulations of the FWT under different incident wind speeds [2].

This method is convenient to implement due to its relative simplicity, and is normally adopted in combination with the frequency-dependent thrust obtained for a fixed wind turbine, installed on the top of the tower. A disadvantage of this approach is that the interactions of the nacelle


Content from this work may be used under the terms of the Creative Commons Attribution 3.0 licence. Any further distribution of this work must maintain attribution to the author(s) and the title of the work, journal citation and DOI.
Published under licence by IOP Publishing Ltd

motions with the blade pitch control system are not considered, an effect that is known to reduce the damping or even render it negative [5, 6, 7], besides introducing an inertia effect [8]. As a consequence, the damping effect can be significantly overpredicted at frequencies close to the controller bandwidth, if the constant coefficient is used.

Control system effects can be included in an FD model by means of linearization of the thrust and torque. The rotor speed is then included as an additional degree of freedom, and the blade-pitch controller can be written in terms of the system states [9].

The objective of the present work is to relate the linearized thrust equations to the above-mentioned inertia and damping effects, providing a visualization of how those effects vary with wind speed and frequency for a given control system.

The aerodynamic inertia and damping coefficients are calculated both from the linearized thrust equations and from simulations where the nacelle is forced to oscillate with different frequencies, under uniform wind. The obtained coefficients are then included in an FD model of a semi-submersible 10 MW FWT. The responses predicted with the different methods for obtaining the coefficients are compared to coupled time-domain simulations, where the thrust is calculated with the blade element momentum (BEM) theory.

Section 2 presents the frequency domain model for the FWT; Section 3 introduces the thrust linearization procedure and provides formulations for the frequency-dependent aerodynamic inertia and damping coefficients; the time-domain simulations are explained in Section 4, and the results are presented in Section 5; final discussions and conclusions are provided in Section 6.

2. Frequency-domain analysis of FWT

The frequency domain model used in the present work consists of three degrees-of-freedom (DOFs), namely surge, heave, and pitch. The potential-theory hydrodynamic model is the same as the one adopted in the time-domain simulations, presented in Section 4. Viscous excitation is neglected, but viscous damping on the platform is added using stochastic linearization of the drag term in Morison's equation, where the standard deviation of the velocity along the length of the columns and pontoons is found using an iteration scheme.

The stiffness matrix includes both hydrostatic restoring and linearized mooring forces. The mooring stiffness matrix is a function of the mean offset, based on static equilibrium between mooring forces and mean thrust.

Transfer functions from wind speed to thrust force, $F_{UT}(\omega)$, are obtained for each mean wind speed as the squared root of the ratio between the spectrum of thrust time series, obtained from simulations with turbulent wind on a fixed turbine, and the incoming wind spectrum. The wind force vector is then found as

$$\mathbf{F}_U(\omega) = \begin{bmatrix} F_{UT}(\omega) & 0 & z_{hub}F_{UT}(\omega) \end{bmatrix}^\top , \tag{1}$$

where z_{hub} is the hub height above still water level (SWL). Transfer functions from wave and wind input to platform response, $\mathbf{H}_{\zeta X}(\omega)$ and $\mathbf{H}_{UX}(\omega)$ respectively, are expressed as

$$\mathbf{H}_{\zeta X}(\omega) = \mathbf{H}_{FX}(\omega)\mathbf{F}_\zeta(\omega),\ \mathbf{H}_{UX}(\omega) = \mathbf{H}_{FX}(\omega)\mathbf{F}_U(\omega)\,, \tag{2}$$

where

$$\mathbf{H}_{FX}(\omega) = \left[-\omega^2(\mathbf{M} + \mathbf{A}(\omega)) + i\omega\mathbf{B}(\omega) + \mathbf{K}\right]^{-1} \tag{3}$$

is the frequency response function matrix. After solving for the platform motions, the tower base bending moment response is found by considering dynamic equilibrium.

Using the wind and wave spectra, the response spectrum for an arbitrary response parameter ξ is then expressed as

$$S_\xi(\omega) = |H_{\zeta\xi}(\omega)|^2 S_\zeta(\omega) + |H_{U\xi}(\omega)|^2 S_U(\omega)\,. \tag{4}$$

3. Aerodynamic damping and inertia effects

The FD model described in Section 2 neglects the variations in the thrust caused by the FWT motions. The interactions between thrust and FWT motions are often represented by a constant damping coefficient, which is added to the matrix **B** in equation (3). This approach neglects the controller action. When the controller is included, its effect results in frequency-dependent damping and inertia coefficients, as shown further below.

3.1. Thrust linearization without controller

A common way to calculate the aerodynamic damping in FD models [1, 4, 3] is to linearize the thrust with respect to the relative wind speed at hub height, v, at different mean incoming wind speeds, U_w, considering no change in the blade pitch angle or rotor speed. Using a first order Taylor series expansion, the thrust is then expressed as

$$T = T_0 + \frac{\partial T}{\partial v}\Delta v\,. \tag{5}$$

Let the nacelle dynamics be represented by an 1-DOF, 1$^{\text{st}}$-order system:

$$m\ddot{x} + c\dot{x} + kx = T\,. \tag{6}$$

Uniform, non-turbulent wind is assumed for now. Recalling that $v = U_w - \dot{x}$, it is noted that $\Delta v = v - U_w = -\dot{x}$. Replacing (5) in (6), the damping effect becomes clear:

$$m\ddot{x} + \left(c + \frac{\partial T}{\partial v}\right)\dot{x} + kx = T_0\,, \tag{7}$$

and the coefficient, b_{aer}, can be expressed as

$$b_{aer} = \frac{\partial T}{\partial v}\,. \tag{8}$$

The damping effect estimated with this method considers the change in the steady-state thrust for a small perturbation in the uniform wind speed seen by the rotor, while neglecting the effect of the control system and rotor dynamics. Different coefficients are obtained for each incident wind velocity, but they are constant with respect to the nacelle frequency of oscillation. This method is relatively simple to use and normally provides satisfactory results when the turbine oscillates in a frequency range distant from the controller bandwidth. For lower frequencies of oscillation, interaction with the control system takes place and the damping coefficient dependence on frequency becomes more important.

3.2. Thrust linearization including controller

A more comprehensive method, which captures effects from the wind turbine controller, may be used by including the rotor speed DOF and control system in the FD model, and also linearizing the thrust with respect to rotor speed, Ω, and blade pitch angle, β:

$$T = T_0 + T_v\Delta v + T_\Omega\Delta\Omega + T_\beta\Delta\beta\,, \tag{9}$$

where the index indicates partial derivative w.r.t. the indicated variable, i.e., $A_B = \frac{\partial A}{\partial B}$. In order to find the damping coefficient, Equation (9) must be written in terms of $\dot{x}$ only. First, the aerodynamic torque, Q, is also given in its linearized version:

$$Q = Q_0 + Q_v\Delta v + Q_\Omega\Delta\Omega + Q_\beta\Delta\beta\,, \tag{10}$$

In addition, the rotor dynamics are given by

$$I_d\dot{\Omega} = Q - N_g E\,, \tag{11}$$

where I_d is the drivetrain inertia, N_g is the gear ratio and E is the electrical (generator) torque, here assumed as constant above rated wind speed. In equilibrium, $Q_0 = N_g E$, so replacing (10) in (11):

$$I_d\dot{\Omega} = Q_v\Delta v + Q_\Omega\Delta\Omega + Q_\beta\Delta\beta\,. \tag{12}$$

It is assumed that a PI controller commands the blade pitch angle, i.e.,

$$\Delta\beta = K_p\Delta\Omega + K_i\int\Delta\Omega dt\,, \tag{13}$$

where K_p and K_i are the proportional and integral controller gains. Equations (9) and (12) are now rewritten replacing $\Delta\beta$ as given in (13), and noting that $\Delta\Omega = \dot{\phi}$, where ϕ is the rotor azimuth angle:

$$T = T_0 - T_v\dot{x} + (T_\Omega + K_pT_\beta)\,\dot{\phi} + K_iT_\beta\phi\,, \tag{14}$$

$$I_d\ddot{\phi} - (Q_\Omega + K_pQ_\beta)\,\dot{\phi} - K_iQ_\beta\phi = -Q_v\dot{x}\,. \tag{15}$$

Assuming harmonic oscillation, Equation (15) can be written in the frequency domain, and the following transfer function between $x(\omega)$ and $\phi(\omega)$ is obtained:

$$\phi(\omega) = \frac{i\omega Q_v}{I_d\omega^2 + (Q_\Omega + K_pQ_\beta)\,i\omega + K_iQ_\beta}x(\omega) = C(\omega)x(\omega)\,. \tag{16}$$

The nacelle dynamics (Equation 6) are now written in terms of T as given in (14), and also expressed in the frequency domain, with $\phi(\omega)$ as given in (16):

$$\left\{-m\omega^2 + i\omega c + k + \underbrace{i\omega T_v - [(T_\Omega + K_pT_\beta)\,i\omega + K_iT_\beta]\,C(\omega)}_{-\omega^2 a_{aer}(\omega) + i\omega b_{aer}(\omega)}\right\}x(\omega) = T_0\,. \tag{17}$$

Based on the assumption that T responds harmonically to harmonic oscillations of the nacelle, the thrust can be written as a combination of terms proportional to the nacelle acceleration and velocity [8]. This assumption is further discussed in Section 3.3, but an immediate consequence is the definition of frequency-dependent, aerodynamic inertia and damping coefficients:

$$a_{aer}(\omega) = -\frac{1}{\omega^2}\,\mathrm{Re}\left\{i\omega T_v - [(T_\Omega + K_pT_\beta)\,i\omega + K_iT_\beta]\,C(\omega)\right\} \tag{18}$$

$$b_{aer}(\omega) = \frac{1}{\omega}\,\mathrm{Im}\left\{i\omega T_v - [(T_\Omega + K_pT_\beta)\,i\omega + K_iT_\beta]\,C(\omega)\right\} \tag{19}$$

3.3. Forced oscillations

The thrust and torque derivatives in Section 3 can be calculated analytically, based on the BEM equations, or numerically, using e.g. the central differences method. Both techniques assume that the thrust and torque respond immediately to changes in v, Ω and β, while in reality the time constants associated with rotor dynamics, aerodynamics, and control system, can be relevant when the nacelle moves at frequencies close to the controller bandwidth.

An alternative method to find the $a_{aer}(\omega)$ and $b_{aer}(\omega)$ coefficients is through simulations of forced nacelle oscillations, with aerodynamics calculated nonlinearly and under influence of

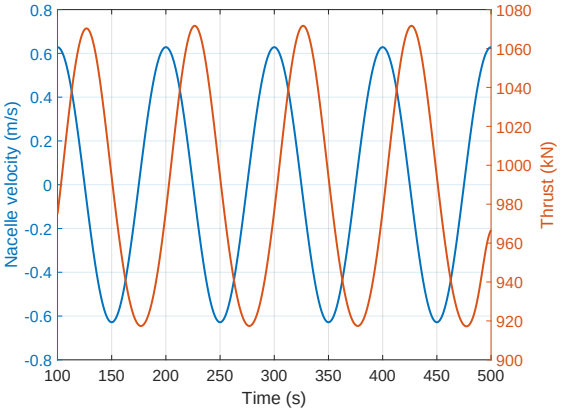

Figure 1: Thrust response to oscillations of the DTU 10 MW wind turbine, under constant incident wind speed of 13.0 m/s and period of oscillation of 100.0 s.

the control system. When the turbine oscillates harmonically, the thrust also oscillates nearly harmonically, but with a phase relative to the nacelle velocity. This can be seen in Figure 1, where the DTU 10 MW wind turbine is forced to oscillate with period 100.0 s and under constant incident wind speed of 13.0 m/s. The thrust can then be assumed to be composed of a mean plus an oscillating component:

$$T = T_0 + T_{osc}(U_w, \omega)\,. \tag{20}$$

Writing the nacelle velocity $\dot{x}$ as

$$\dot{x} = v_0 \cos(\omega t)\,, \tag{21}$$

the oscillating part of the thrust can then be assumed to be given by [8]

$$\begin{aligned} T_{osc} &= f_0 v_0 \cos(\omega t + \alpha) \\ &= f_0 \left[v_0 \cos(\omega t)\cos(\alpha) - v_0 \sin(\omega t)\sin(\alpha)\right] \\ &= f_0 \cos(\alpha)\dot{x} + \frac{f_0 \sin(\alpha)}{\omega}\ddot{x}\,. \end{aligned} \tag{22}$$

The amplifying factor f_0 and the phase α between nacelle velocity and thrust depend on the dynamic effects mentioned above, and are not straightforward to determine analytically. However, for a given turbine and control system they vary with the incident wind speed and frequency of oscillation, while motion amplitude does not seem to have a significant influence. They can therefore be obtained from forced oscillations covering the ranges of interest for both parameters. Fast Fourier transforms (FFTs) of the nacelle velocity and thrust are calculated, and f_0 and α can be directly obtained from the ratio between amplitudes or phases of both FFTs at the period of interest. Formulations for the aerodynamic inertia and damping coefficients are then directly determined from equation (23):

$$a_{aer}(U_w, \omega) = -\frac{f_0 \sin(\alpha)}{\omega}\,, \quad b_{aer}(U_w, \omega) = -f_0 \cos(\alpha)\,, \tag{23}$$

3.4. Coefficients calculation and comparison

The aerodynamic inertia and damping coefficients were obtained both from the linearized thrust and the forced oscillations method. For the former case, the thrust and torque derivatives were

obtained from the linearized BEM equations. For the latter, forced oscillations of the DTU 10 MW wind turbine were performed with a simulator which obtains aerodynamic loads from AeroDyn [10], updates the blade pitch angle based on the same controller strategy presented in Section 4, and updates the rotor speed based on the rotor dynamics as in Equation (11). Oscillation periods varied from 20.0 s to 130.0 s, and uniform wind with the three velocities in Table 3 was considered. The BEM formulation with dynamic stall is adopted for the AeroDyn calculations.

The coefficients obtained with both approaches are shown in Figures 2 and 3. In spite of the oscillatory character of the curves obtained with the oscillation method, the agreement between both methods looks satisfactory, especially for higher wind velocities. The inertia effect is of the order of 1% of the mass of typical FWTs, resulting in negligible consequences for the surge dynamics. The contribution to the moment of inertia in pitch is however considerable, due to the nacelle height. Important changes in the pitch natural period can then result, as shown in [8]. The constant damping coefficients as obtained in equation (5) are also plotted in Fig. 3, showing that the discrepancy w.r.t. the frequency-dependent coefficients is larger for lower frequencies and higher wind velocities.

3.5. The aerodynamic inertia and damping effects on the FWT dynamics

It was already shown that the fluctuations in the aerodynamic thrust resulting from the nacelle motions may be treated as frequency-dependent inertia and damping effects. The derivation assumed non-turbulent wind, under the hypothesis that the fluctuations in the apparent wind flow in the rotor due to turbulence can be decoupled from those caused by the nacelle motions.

Under the same assumption, the fluctuations in the thrust due to nacelle oscillations can now be added to the FD model presented in Section 2. This is done by noting that, from Equations (22) and (23), the oscillating component of the thrust can be written as

$$T_{osc} = -a_{aer}\ddot{x} - b_{aer}\dot{x}\,. \tag{24}$$

The following aerodynamic and damping matrices, $\mathbf{A_{aer}}$ and $\mathbf{B_{aer}}$, are then defined:

$$\mathbf{A_{aer}}(\omega) = \begin{bmatrix} a_{aer}(\omega) & 0 & a_{aer}(\omega)z_{hub} \\ 0 & 0 & 0 \\ a_{aer}(\omega)z_{hub} & 0 & a_{aer}(\omega)z_{hub}^2 \end{bmatrix}, \quad \mathbf{B_{aer}}(\omega) = \begin{bmatrix} b_{aer}(\omega) & 0 & b_{aer}(\omega)z_{hub} \\ 0 & 0 & 0 \\ b_{aer}(\omega)z_{hub} & 0 & b_{aer}(\omega)z_{hub}^2 \end{bmatrix}. \tag{25}$$

$\mathbf{A_{aer}}$ and $\mathbf{B_{aer}}$ are now summed to $\mathbf{A}$ and $\mathbf{B}$ in equation (3), which includes the effect of nacelle motion in the FD analysis.

4. Simulations

The platform considered is the OO-Star 10 MW [11], a semi-submersible concept designed for the LIFES50+ project. The main properties are summarized in Table 1. The potential-theory hydrodynamic loads are generated with WADAM, and viscosity is added in form of the Morison drag term. The platform is installed at a water depth of 130.0 m, and the mooring system consists on a simplified 3-catenary line arrangement, which differs from the original of taut lines with clump weights.

The DTU 10 MW turbine (Table 2) is installed at the top of the tower, at a height of 118.4 m. The blade-pitch controller corresponds to the PI formulation of Equation (13), i.e., the power error contribution of the original controller [12] is not included. The controller gains are tuned such that its bandwidth is below the pitch natural period, and a gain scheduling strategy corrects the gains according to the current blade pitch angle.

The time-domain simulations were performed with SIMA, a workbench which allows for coupled analyses between floating bodies and slender elements [14, 15]. The platform, nacelle

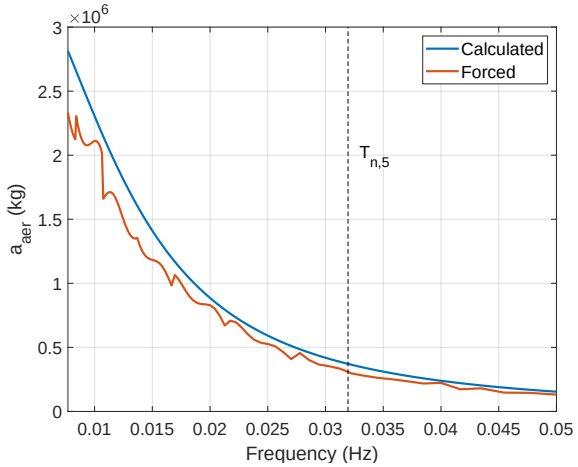

(a) $U_w = 13.0$ m/s.

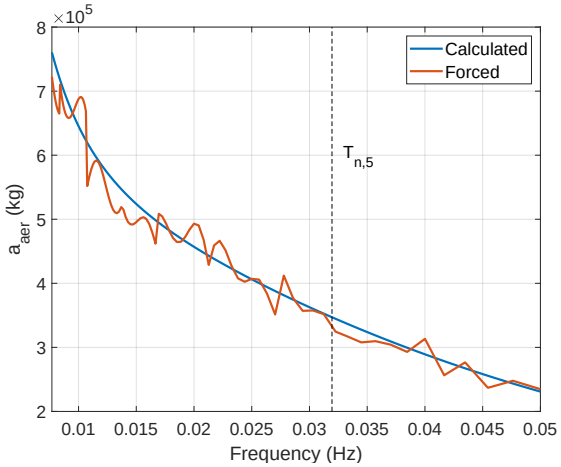

(b) $U_w = 19.0$ m/s.

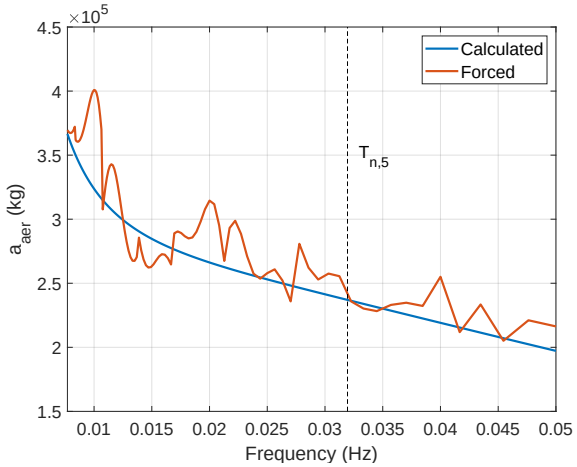

(c) $U_w = 25.0$ m/s.

Figure 2: Aerodynamic inertia coefficients, calculated with the linearized approach or obtained from the forced oscillations method.

Draft, D (m)	22.0
Total mass, m_{tot} (kg)	2.36×10^7
Center of gravity, VCG (m)	-7.9
Surge nat. per., T_1 (s)	181.8
Pitch nat. per., T_5 (s)	31.3

Table 1: Main properties of the OO-Star 10 MW FWT [11].

and hub are modeled as rigid bodies, while the blades, tower and mooring lines are modeled as flexible structures, with finite elements. The aerodynamics are based on the BEM theory, with dynamic stall and dynamic wake effects based on Øye's models [16]. Hub and tip losses are modeled with the Prandtl factor, and Glauerts correction is applied for high induction factors. The environmental conditions are listed in Table 3. Turbulent wind was generated with TurbSim [17], using the IEC Kaimal spectrum with turbulence characteristic B (moderate). A JONSWAP

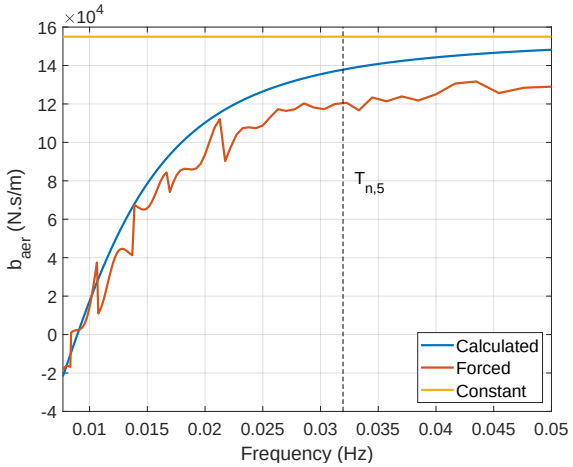

(a) $U_w = 13.0$ m/s.

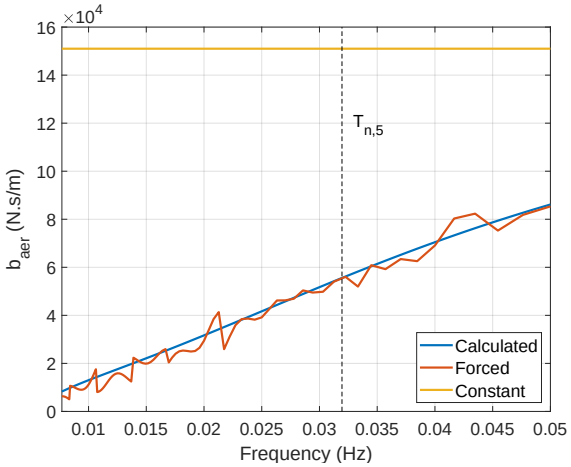

(b) $U_w = 19.0$ m/s.

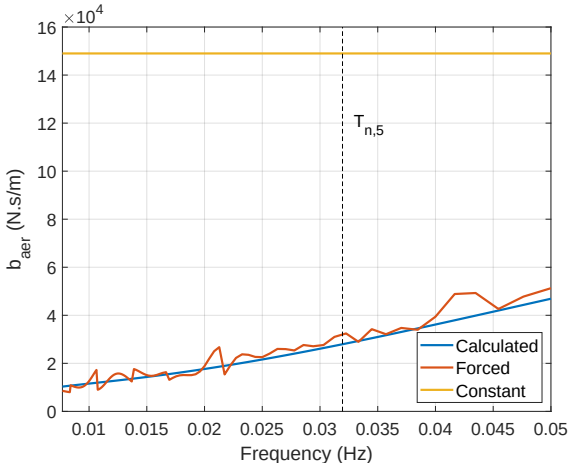

(c) $U_w = 25.0$ m/s.

Figure 3: Aerodynamic damping coefficients, calculated with the linearized approach (both constant and frequency-dependent) or obtained from the forced oscillations method.

Rotor radius, R (m)	89.2
Rated rotor speed, Ω_0 (rad/s)	1.0
Drivetrain inertia, I_d (kg.m^2)	1.6×10^8
Gear ratio, N_g (-)	50
Rotor-nacelle assemble mass, m_{RNA} (kg)	6.7×10^5
Proportional controller gain, K_p (s)	0.1794
Integral controller gain, K_i (-)	0.0165

Table 2: Main properties of the DTU 10MW wind turbine [13]. The controller gains refer to $\beta = 0°$.

wave spectrum with a γ factor of 3.3 was used to describe the sea state. The simulations lasted for one hour, which showed to provide a sufficient number of LF oscillations for the analysis. Only one realization of each condition was considered.

	U_w (m/s)	H_s (m)	T_p (s)
C1	13.0	2.7	10.3
C2	19.0	4.0	11.1
C3	25.0	5.8	12.1

Table 3: Environmental conditions.

5. Results

Figure 4 shows the frequency-domain pitch response for the three conditions in Table 3, obtained with time-domain simulations in SIMA; and with the FD model from Section 2, using the different approaches for including the aerodynamic damping and inertia effects, as presented in Section 3. When the constant damping coefficient from Equation (8) is adopted, the method is referred to as *FD constant*; with the frequency-dependent inertia and damping coefficients as given by Equations (18) and (19), the approach is named *FD calculated*; and when the coefficients are obtained from the forced harmonic oscillations, as in Equation (23), the *FD forced* identifier is adopted.

The curves indicate that the adoption of a constant damping coefficient overestimates the damping effect at lower frequencies, resulting in significantly underpredicted resonant response for frequencies below 0.05 Hz. When frequency-dependent coefficients are adopted, however, the situation is the opposite: the damping effect is underestimated, resulting in higher response for lower frequencies. Using the coefficients based on the forced oscillations leads to improved results in comparison with those obtained from the linearized thrust equations, in terms of the pitch motion standard deviation (Table 4). All three methods perform equivalently in the wave-frequency range (0.05-0.15 Hz), where the response is underpredicted due to the absence of viscous excitation in the FD model.

Similar conclusions can be obtained regarding the tower-base bending moment (Figure 5). The most remarkable difference in comparison with the plots for the pitch response is for $U_w =$ 13.0 m/s (Figure 5a), which shows a persistent underprediction for all the three FD models for frequencies above 0.04 Hz. The errors in predicted tower base bending moment, shown in Table 4, are in general lower than for the pitch motion, since wave-frequency and 3p loads also influence the tower-base bending moment, and are less affected by the damping dependence of frequency. The accuracy is satisfactory for calculated and, especially, forced methods.

Figure 6 compares the low-frequency responses in pitch, for $U_w = 19.0$ m/s, when the inertia effect is included or disregarded. The FD model with damping coefficient obtained from forced oscillations is adopted, but only the blue curve includes the inertia coefficient – resulting in a peak period about 2.5 s longer then when the inertia effect is not considered.

6. Conclusion

A method was developed to illustrate the importance of including the interaction between the nacelle motions and thrust in the frequency-domain representation of a FWT. The thrust fluctuations resulting from nacelle motions can be interpreted as frequency-dependent inertia and damping effects, which challenges the traditional approach of adopting a constant aerodynamic damping coefficient.

Expressions were derived for the respective coefficients based both on a linearized expression for the thrust and on forced oscillations of a wind turbine in the time domain. The obtained coefficients were included in a 3 DOF FD model of the OOstar semi-submersible FWT. Comparisons were made between the models using a constant aerodynamic damping coefficient, the frequency-dependent inertia and damping coefficients obtained in two different ways, and

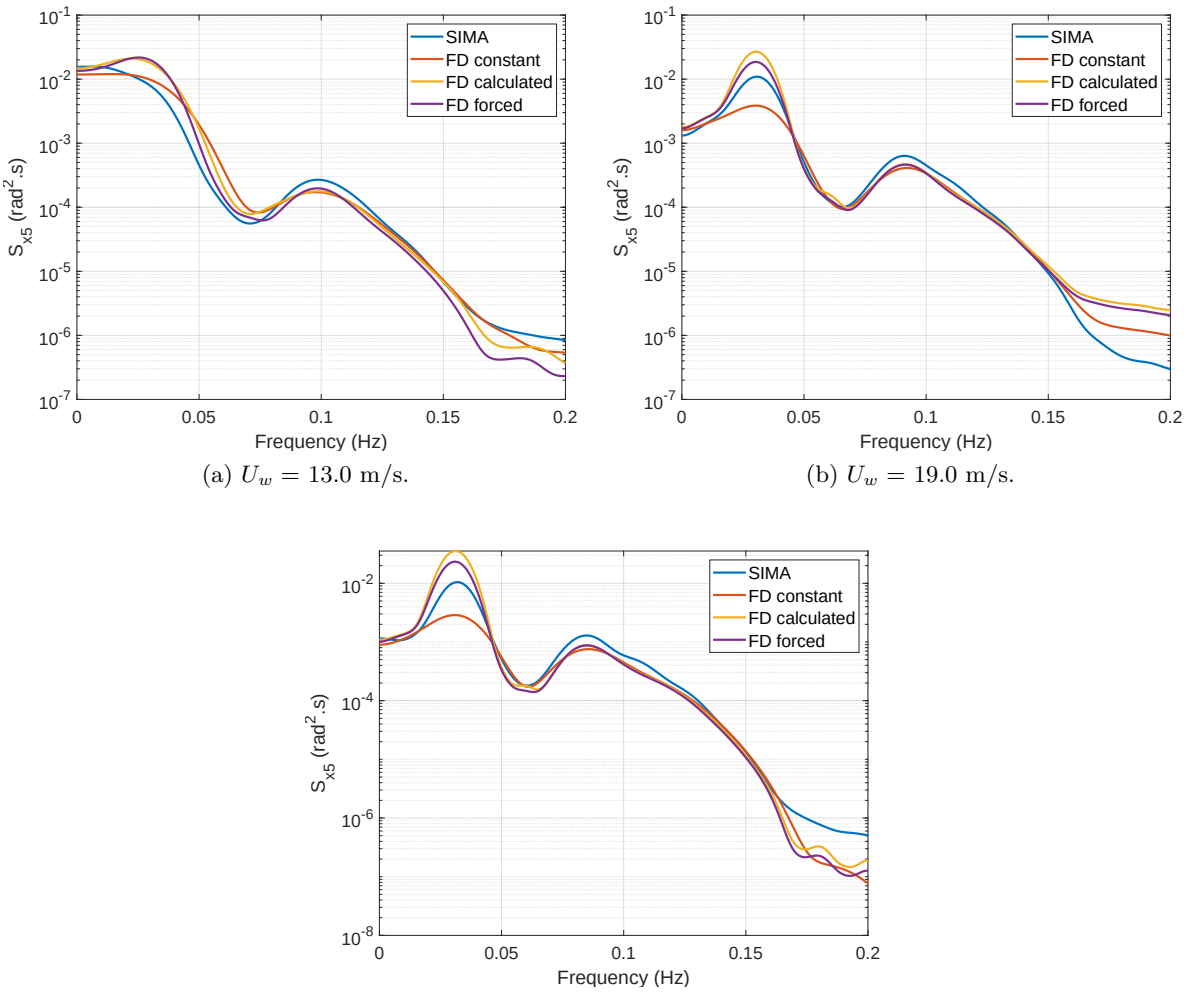

(a) $U_w = 13.0$ m/s.

(b) $U_w = 19.0$ m/s.

(c) $U_w = 25.0$ m/s.

Figure 4: Frequency-domain platform pitch response – comparison between SIMA simulations and frequency-domain analyses with different approaches for calculating the aerodynamic inertia and damping.

time-domain simulations. Both platform pitch motion and tower base bending moment were analyzed. It was observed that the constant damping coefficient underestimates the responses in the frequency range of the FWT surge and pitch natural frequencies.

The frequency-dependent coefficients, on the other hand, overestimated the response in the same frequency range, but are closer to the time-domain predictions. The aerodynamic inertia was shown to increase the pitch natural period by about 2.5 s, for a mean incident wind speed of 19.0 m/s. The differences between using coefficients based on the linearized thrust or on the forced oscillations were not very significant, but a slightly better agreement of the LF responses with the time-domain simulations was attained with the latter.

The introduction of inertia and damping coefficients was chosen for its didactic interest, but the adoption of a linearized thrust as in Equation (9) in a FD model is a simpler and equivalent approach to include the interaction between nacelle motion and thrust, with due consideration of controller and rotor dynamic effects.

In any case, a better agreement of the LF response should still be pursued. Other linearization

Condition	FD constant (%)	FD calculated (%)	FD forced (%)
C1	-0.2	+23.7	+21.8
C2	-24.8	+38.0	+20.0
C3	-29.6	+55.0	+30.6

Table 4: Error in pitch standard deviation compared to time domain simulations.

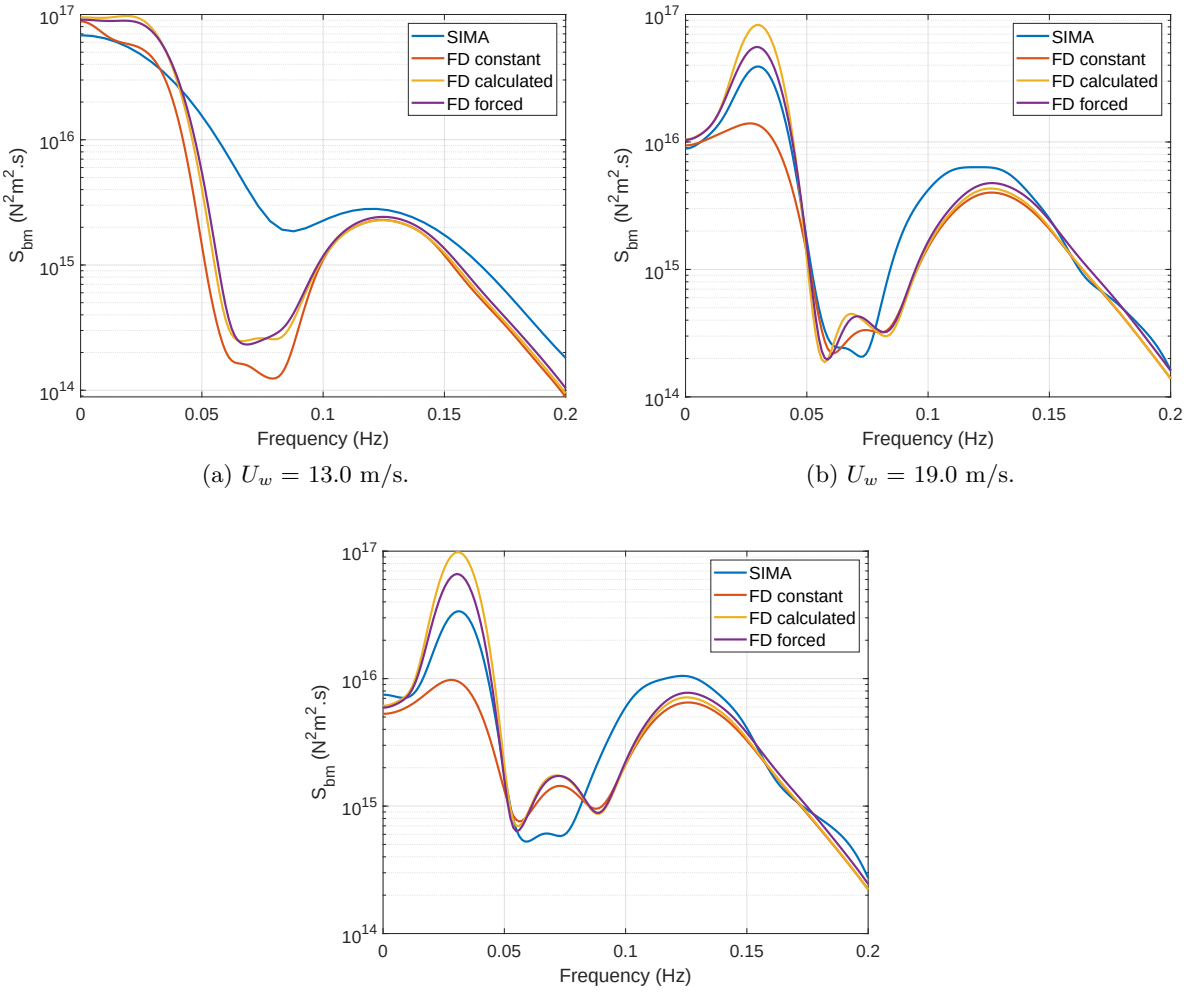

(a) $U_w = 13.0$ m/s.

(b) $U_w = 19.0$ m/s.

(c) $U_w = 25.0$ m/s.

Figure 5: Frequency-domain tower base bending moment – comparison between SIMA simulations and frequency-domain analyses with different approaches for calculating the aerodynamic inertia and damping.

methods could be attempted, trying to preserve effects other than those obtained with the partial derivatives of thrust and torque w.r.t. relative wind velocity, rotor speed and blade-pitch angle.

Condition	FD constant (%)	FD calculated (%)	FD forced (%)
C1	-7.1	+13.0	+10.7
C2	-29.8	+15.1	+2.9
C3	-33.0	+19.2	+5.3

Table 5: Error in tower base bending moment standard deviation compared to time domain simulations.

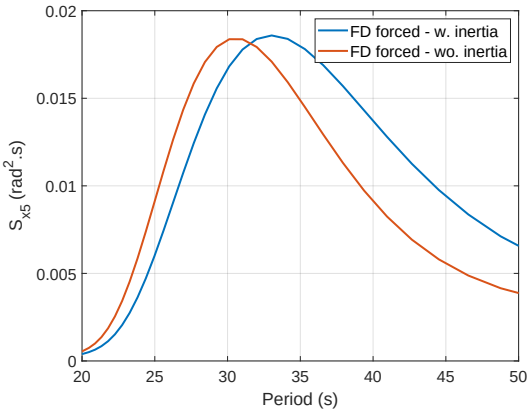

Figure 6: Pitch response estimated in the frequency domain for $U_w = 19.0$ m/s, with aerodynamic damping estimated using the forced oscillations method and with/without considering the aerodynamic inertia effect.

References

[1] Kvittem MI, Moan T. Frequency Versus Time Domain Fatigue Analysis of a Semisubmersible Wind Turbine Tower. Journal of Offshore Mechanics and Arctic Engineering. 2015 Feb;137(1):011901–011901–11. Available from: http://dx.doi.org/10.1115/1.4028340.

[2] Pegalajar-Jurado A, Borg M, Bredmose H. An efficient frequency-domain model for quick load analysis of floating offshore wind turbines. Wind Energy Science. 2018;3(2):693–712. Available from: https://www.wind-energ-sci.net/3/693/2018/.

[3] Hegseth JM, Bachynski EE. A semi-analytical frequency domain model for efficient design evaluation of spar floating wind turbines. Marine Structures. 2019;64:186 – 210. Available from: http://www.sciencedirect.com/science/article/pii/S0951833918303149.

[4] Bachynski EE. Design and dynamic analysis of tension leg platform wind turbines [Ph.D. thesis]. Norwegian University of Science and Technology. Trondheim, Norway; 2014.

[5] Nielsen F, Hanson T, Skaare B. Integrated dynamic analysis of floating offshore wind turbines. In: Proceedings of the ASME 2016 25th International Conference on Offshore Mechanics and Arctic Engineering; 2006. .

[6] Larsen TJ, Hanson TD. A method to avoid negative damped low frequent tower vibrations for a floating, pitch controlled wind turbine. Journal of Physics: Conference Series. 2007 jul;75:012073. Available from: https://doi.org/10.1088%2F1742-6596%2F75%2F1%2F012073.

[7] Jonkman JM. Influence of control on the pitch damping of a floating wind turbine. In: Proceedings of the ASME Wind Energy Symposium; 2008. .

[8] Souza CES, Bachynski EE. Changes in surge and pitch decay periods of floating wind turbines for varying wind speed. Ocean Engineering. 2019;180:223 – 237. Available from: http://www.sciencedirect.com/science/article/pii/S0029801818315932.

[9] Goupee AJ, Kimball RW, Dagher HJ. Experimental observations of active blade pitch and generator control influence on floating wind turbine response. Renewable Energy. 2017;104:9 – 19.

[10] Moriarty PJ, Hansen AC. AeroDyn Theory Manual. Denver, Colorado: National Renewable Energy

Laboratory; 2005. NREL/EL-500-36881.
[11] Müller K, Lemmer F, Yu W. LIFES50+ - D4.2 Public Definition of the Two LIFES50+ 10MW Floater Concepts. University of Stuttgart; 2018.
[12] Hansen MH, Henriksen LC. Basic DTU Wind Energy controller. Technical University of Denmark; 2019. DTU Wind Energy E No. 0028.
[13] Bak C, Zahle F, Bitsche R, Kim T, Yde A, Henriksen LC, et al. Description of the DTU 10 MW Reference Wind Turbine. DTU Wind Energy; 2013. DTU Wind Energy Report-I-0092.
[14] SINTEF OCEAN. RIFLEX - Theory manual; 2016.
[15] SINTEF OCEAN. SIMO - Theory manual; 2016.
[16] Hansen MOL. Aerodynamics of Wind Turbines. Earthscan; 2013.
[17] Jonkman BJ, Kilcher L. TurbSim User's Guide: version 1.06.00. National Renewable Energy Laboratory; 2012.